coupling. The excitation power used in the strong coupling experiments of 2 μW corresponds to 1.5×10^9 photons s^{-1} in the cavity averaged over time; that is, interactions of the single QD with multiple photons can be neglected.

Our experiments demonstrate that long-sought solid state implementations of the strongly coupled cavity-mode–two-level-emitter systems are feasible by using single QDs in high-*Q* cavities with small mode volumes. With further improvements, for example using higher-*Q* cavities or QDs placed at the in-plane mode centre, these systems have the potential for wide application ranging from nonlinear optics[28] to quantum information processing[18–22]. □

Received 11 June; accepted 26 August 2004; doi:10.1038/nature02969.

1. Yamamoto, Y. & Slusher, R. E. Optical processes in microcavities. *Physics Today* **46,** 66–73 (1993).
2. Gerard, J. M. & Gayral, B. InAs quantum dots: artificial atoms for solid-state cavity-quantum electrodynamics. *Physica E* **9,** 131–139 (2001).
3. Vahala, K. J. Optical microcavities. *Nature* **424,** 839–846 (2003).
4. Kleppner, D. Inhibited spontaneous emission. *Phys. Rev. Lett.* **47,** 233–236 (1981).
5. Goy, P., Raimond, J. M., Cross, M. M. & Haroche, S. Observation of cavity-enhanced single-atom spontaneous emission. *Phys. Rev. Lett.* **50,** 1903–1906 (1983).
6. Gabrielse, G. & Dehmelt, H. Observation of inhibited spontaneous emission. *Phys. Rev. Lett.* **55,** 67–70 (1985).
7. Hulet, R. G., Hilfer, E. S. & Kleppner, D. Inhibited spontaneous emission by a Rydberg atom. *Phys. Rev. Lett.* **55,** 2137–2140 (1985).
8. Gerard, J. M. *et al.* Enhanced spontaneous emission by quantum boxes in a monolithic optical microcavity. *Phys. Rev. Lett.* **81,** 1110–1113 (1998).
9. Bayer, M. *et al.* Inhibition and enhancement of the spontaneous emission of quantum dots in structured microresonators. *Phys. Rev. Lett.* **86,** 3168–3171 (2001).
10. Solomon, G. S., Pelton, M. & Yamamoto, Y. Single-mode spontaneous emission from a single quantum dot in a three-dimensional microcavity. *Phys. Rev. Lett.* **86,** 3903–3906 (2001).
11. Pelton, M. *et al.* Efficient source of single photons: a single quantum dot in a micropost microcavity. *Phys. Rev. Lett.* **89,** 233602-1-4 (2002).
12. Santori, C., Fattal, D., Vuckovic, J., Solomon, G. S. & Yamamoto, Y. Indistinguishable photons from a single-photon device. *Nature* **419,** 594–597 (2002).
13. Michler, P. *et al.* A quantum dot single-photon turnstile device. *Science* **290,** 2282–2285 (2000).
14. Hood, C. J., Chapman, M. S., Lynn, T. W. & Kimble, H. J. Real-time cavity QED with single atoms. *Phys. Rev. Lett.* **80,** 4157–4160 (1998).
15. Mabuchi, H. & Doherety, A. C. Cavity quantum electrodynamics: coherence in context. *Science* **298,** 1372–1377 (2002).
16. McKeever, J. *et al.* Experimental realization of one-atom laser in the regime of strong coupling. *Nature* **425,** 268–271 (2003).
17. McKeever, J. *et al.* State-insensitive cooling and trapping of single atoms in an optical cavity. *Phys. Rev. Lett.* **90,** 133602-1-4 (2003).
18. Monroe, C. Quantum information processing with atoms and photons. *Nature* **416,** 238–246 (2002).
19. Imamoglu, A. *et al.* Quantum information processing using quantum dot spins and cavity QED. *Phys. Rev. Lett.* **83,** 4204–4207 (1999).
20. Stievater, T. H. *et al.* Rabi oscillations of excitons in single quantum dots. *Phys. Rev. Lett.* **87,** 133603-1-4 (2001).
21. Li, X. Q. & Yan, Y. J. Quantum computation with coupled quantum dots in optical microcavities. *Phys. Rev. B* **65,** 205301-1-5 (2002).
22. Kiraz, A., Atatüre, M. & Imamoglu, A. Quantum-dot single-photon sources: Prospects for applications in linear optics quantum-information processing. *Phys. Rev. A.* **69,** 032305 (2004).
23. Andreani, L., Panzarini, G. & Gerard, J. M. Strong-coupling regime for quantum boxes in pillar microcavities: Theory. *Phys. Rev. B* **60,** 13276–13279 (1999).
24. Rudin, S. & Reinecke, T. L. Oscillator model for vacuum Rabi splitting in microcavities. *Phys. Rev. B* **59,** 10227–10233 (1999).
25. Purcell, E. M. Spontaneous emission probabilities at radio frequencies. *Phys. Rev.* **69,** 681 (1946).
26. Bayer, M. & Forchel, A. Temperature dependence of the exciton homogeneous linewidths in $In_{0.6}Ga_{0.4}As/GaAs$ self-assembled quantum dots. *Phys. Rev. B* **65,** 041308-1-4 (R) (2002).
27. Guest, J. R. *et al.* Measurement of optical absorption by a single quantum dot exciton. *Phys. Rev. B* **65,** 241310-1-4 (2002).
28. Shimizu, Y. *et al.* Control of light pulse propagation with only a few cold atoms in a high finesse microcavity. *Phys. Rev. Lett.* **89,** 233001-1-4 (2002).

Supplementary Information accompanies the paper on **www.nature.com/nature**.

Acknowledgements Partial financial support of this work by the DARPA QuIST program, the Deutsche Forschungsgemeinschaft via Research Group Quantum Optics in Semiconductor Nanostructures, the Office of Naval Research and the ONR Nanoscale Electronics Program, INTAS and the State of Bavaria is acknowledged.

Competing interests statement The authors declare that they have no competing financial interests.

Correspondence and requests for materials should be addressed to A.F. (alfred.forchel@physik.uni-wuerzburg.de).

Vacuum Rabi splitting with a single quantum dot in a photonic crystal nanocavity

T. Yoshie[1], A. Scherer[1], J. Hendrickson[2], G. Khitrova[2], H. M. Gibbs[2], G. Rupper[2], C. Ell[2], O. B. Shchekin[3] & D. G. Deppe[3]

[1]*Electrical Engineering, California Institute of Technology, Pasadena, California 91125, USA*
[2]*Optical Sciences Center, The University of Arizona, Tucson, Arizona 85721, USA*
[3]*Microelectronics Research Center, Department of Electrical and Computer Engineering, The University of Texas at Austin, Austin, Texas 78712, USA*

Cavity quantum electrodynamics (QED) systems allow the study of a variety of fundamental quantum-optics phenomena, such as entanglement, quantum decoherence and the quantum–classical boundary[1–9]. Such systems also provide test beds for quantum information science. Nearly all strongly coupled cavity QED experiments have used a single atom in a high-quality-factor (high-*Q*) cavity. Here we report the experimental realization of a strongly coupled system in the solid state: a single quantum dot embedded in the spacer of a nanocavity, showing vacuum-field Rabi splitting exceeding the decoherence linewidths of both the nanocavity and the quantum dot. This requires a small-volume cavity and an atomic-like two-level system[5,10]. The photonic crystal[11] slab nanocavity—which traps photons when a defect is introduced inside the two-dimensional photonic bandgap by leaving out one or more holes[12]—has both high *Q* and small modal volume *V*, as required for strong light–matter interactions[13]. The quantum dot has two discrete energy levels with a transition dipole moment much larger than that of an atom[14–16], and it is fixed in the nanocavity during growth.

The study of vacuum Rabi splitting has been an exciting subfield of atomic physics since its first observation with many atoms in the early 1980s; see ref. 1 for a history of the field. After a decade of gradually improving the *Q* of the cavity and decreasing its volume, vacuum Rabi splitting was seen with a single atom. This opened exciting opportunities for the field of atomic cavity QED, and many experiments followed[1–7]. For such a truly quantum system, the optical properties are changed by the addition of a single photon or single atom, and the quantum–classical boundary can be studied[2–4]. But because atoms can move and even escape, their coupling is time-dependent; clearly, the next goal was to localize a cold atom inside the cavity using atomic traps[6].

In the field of semiconductors, 12 years elapsed between seeing non-perturbative normal mode coupling[17], analogous to many-atom vacuum Rabi splitting[10], and the observation of strong coupling between a single quantum dot (SQD) and a small-volume crystal nanocavity. This advance, which produced opportunities for truly quantum-optics cavity QED experiments in semiconductors, owes much to the extensive studies of (and improvements in) SQDs and monolithic cavities. The semiconductor approximation to a two-level system is a SQD, a small semiconductor crystal confined in three dimensions by a higher-bandgap material[14–16]. The sharp emission lines observed from submicrometre collection spots were shown to arise from transitions between discrete energy levels of the quantum dot (QD) depending upon size and shape[18,19]. Coherent transient experiments were performed on these atom-like transitions[16,20], and their spontaneous emission was enhanced[21–23] and inhibited[22] by the Purcell effect within microcavities[24] of higher and higher *Q*. The transitions of a SQD can be separated enough for the lowest transition to exhibit anti-bunching, and cavity enhanced spontaneous emission can lead to one photon on demand into a desired mode[21,25].

The condition for strong coupling is more demanding on Q: the vacuum Rabi splitting, $2g$, due to a SQD must exceed the mean of the decay rates of the cavity, κ, and the dot, γ. The coupling strength, g, is given by $\mu E_{vac}/h$, where the vacuum field satisfies $n^2\varepsilon_0|E_{vac}|^2V = h\nu/2$. Here $n \approx 3.4$ is the semiconductor refractive index, ε_0 is the permittivity of vacuum, V is the mode volume, and ν is the frequency of the transition of the quantum dot with dipole moment μ. For small-length cavities, $\kappa(=\nu/Q)$ usually exceeds γ; then, since $g/\kappa \propto Q/\sqrt{V}$, the challenge has been to fabricate a high-Q cavity while maintaining a very small V. Recently, a breakthrough in design by Noda's group[13] resulted in silicon photonic crystal nanocavities with $Q = 45{,}000$ and $V = 0.07\,\mu m^3$. Clearly, the cavity with the smallest V (while maintaining high Q) yields strong coupling with a smaller dipole, that is, the dot is more quantum.

Our photonic crystal nanocavity follows the design[13] of Noda's group, but the silicon is replaced by GaAs for growth of quantum dots. The three-dimensional-mode in-plane confinement is obtained by fabricating a two-dimensional triangular lattice photonic crystal slab with three holes missing to form a spacer (Fig. 1a, b). The vertical confinement, achieved by total internal reflection at the slab semiconductor–air interfaces, is imperfect, in that light with small in-plane wavevectors can leak out of the top and bottom. Noda's one-dimensional model showed that the key to reducing this loss is to shift out slightly the holes at the ends of the spacer: "the light has to be confined gently in order to confine it strongly"[13]. In other words, when the field envelope function is stopped abruptly, its Fourier transform has a larger overlap with small in-plane wavevectors that leak out; terminating it gently reduces that loss[13].

The sample, grown on a (001) GaAs substrate by molecular beam epitaxy, has a single layer of InAs quantum dots in the centre of the slab[26] (Fig. 2a). A large array of nanocavities (~30,000 in clusters of 30 with a density of 5,560 cavities mm^{-2}) is fabricated with crystal parameters changed systematically. The missing-holes spacer is surrounded by 14 periods of air holes for good in-plane optical confinement. The parameters of the photonic crystal are controlled lithographically[26]: $a = 300$ nm, $r = 0.27a$, $s = 0.20a$, and slab thickness $d = 0.90a$ (see Fig. 1b for definitions of a, r and s).

Computations of the field strength as a function of position (Fig. 1c) show that most of the field energy is confined to the defect region with a mode volume of $V \approx (\lambda_0/n)^3 \approx 0.04\,\mu m^3$, where λ_0 is the resonance wavelength of light in vacuum. This V is a typical value for most of the parameter ranges. Since the intracavity field is a standing wave that oscillates from zero to a maximum every quarter wavelength (see top of Fig. 1c), there is a very limited volume of high field strength in which a SQD must be located if it is to couple strongly.

Photoluminescence (PL) measurements were performed in a temperature-controlled liquid-helium cryostat with internal x–y nanopositioners, essential for stability and the ability to re-find a

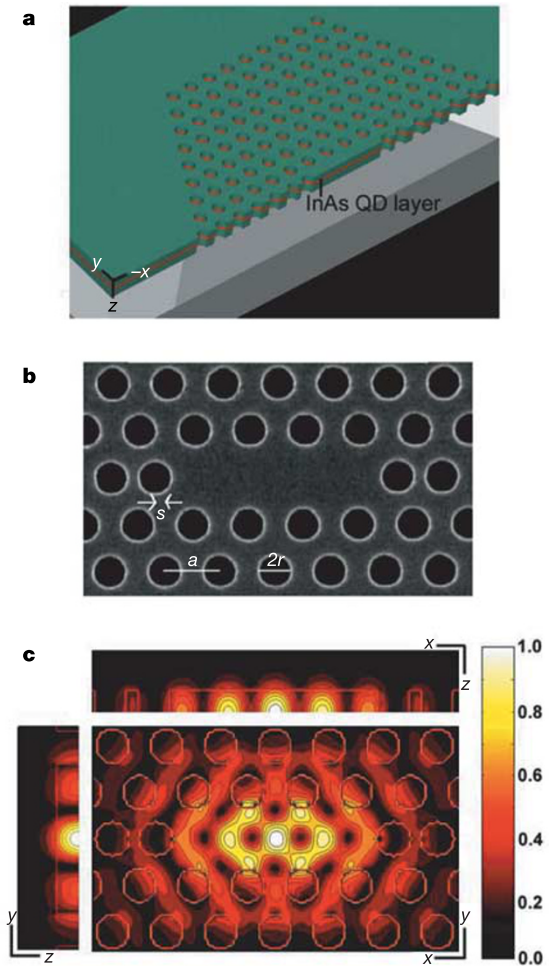

Figure 1 Photonic crystal nanocavity. **a**, Diagram. Half of a hexagon-shaped array of holes forming a nanocavity; scale is ~5 μm across at the cut. **b**, Scanning electron micrograph of a fabricated nanocavity, showing the hole spacing a, hole diameter $2r$, and shift s of the two holes at the ends of the 'spacer' formed by omitting three holes. **c**, Computed optical field magnitude superimposed on the nanocavity structure. The scale bar shows the normalized amplitude of the electric field, $|E|/\max(|E|)$. Also shown are a horizontal slice (above main panel) and a vertical slice (left of main panel) through the centre of the spacer.

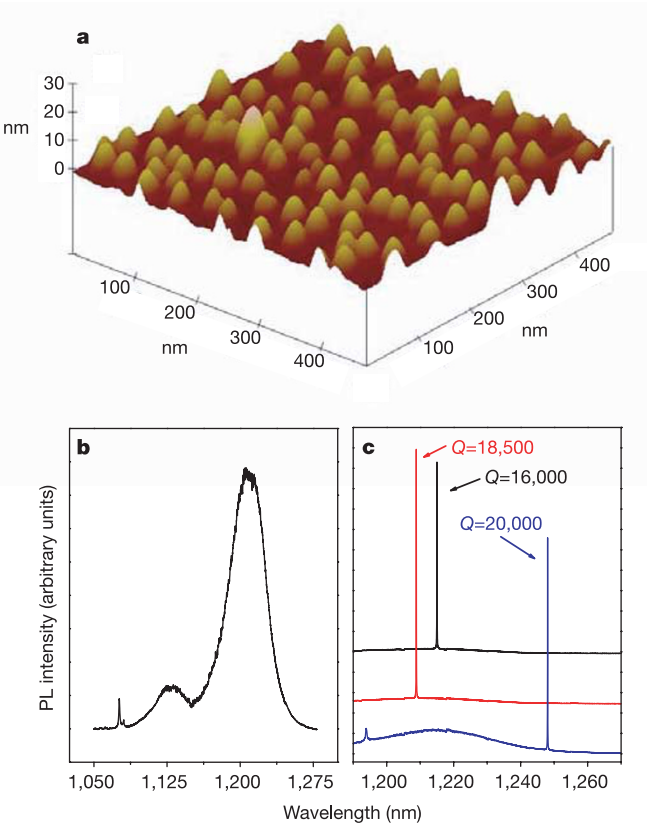

Figure 2 Quantum dots and cavity modes. **a**, Atomic force microscope profile of a layer of InAs QDs similar to the layer used but without layers above. The typical dot size is ~25 nm diameter and 3–4 nm height, and the dot density is 300–400 μm^{-2}. **b**, QD ensemble photoluminescence for high excitation power, showing both the lowest (1,175–1,250 nm) and first excited (1,100–1,150 nm) transitions. **c**, PL from the three nanocavities with the highest values of Q (uncorrected for ~0.04-nm instrument width). Averaging time: 0.1 s for left two peaks; 0.5 s for right.

given nanocavity. The samples were optically pumped by the 770 nm output of a Ti:sapphire continuous wave (c.w.) laser. The pump beam was focused by a reflecting microscope objective (0.5 numerical aperture) to a spot size of 1 μm on the sample. The sample emission was collected by the same microscope objective, analysed with a spectrometer, and detected by an InGaAs array integrating over 0.025 nm per pixel. We estimate that a sample area of ~10 μm^2 is imaged into the spectrometer, giving rise to the broad ensemble PL underlying the cavity-related emission in Figs 3 and 4. In this geometry we are using the leakage of the cavity mode out of the top to observe PL from a QD coupled to it. Figure 2b shows the ensemble PL spectrum with the lowest transition line at ~1,200 nm, and the first excited transition line at 1,125 nm. Figure 2c shows high-power spectra of the three highest-Q nanocavities. There has been a steady improvement in the values of Q obtained for two-dimensional photonic crystal slab nanocavities[12,13,26] fabricated for lasers, with a quantum well[12] ($Q = 250$) or ~80 quantum dots[26] ($Q = 2{,}000$) as the active medium.

We did not find a SQD coupled strongly to one of the highest-Q modes displayed in Fig. 2c. But a slightly lower-Q (~13,300) mode does couple to a SQD located spectrally on the short wavelength side of the lowest energy transition of the ensemble shown in Fig. 2b. At high power (Fig. 3a as in Fig. 2c), the emission is dominated by the cavity peak, because QDs not coupled to the nanocavity are saturated; that is, a QD's emission rate is determined by its radiative decay rate, not by its excitation rate. Therefore, coupled dots emit more photons per unit time than uncoupled dots, owing to Purcell enhancement of spontaneous emission[23]. A time-resolved experiment would be needed to see the faster decay of a coupled dot.

At intermediate power (25 μW), the increased QD absorption reduces the Q to 8,000. At low power (Fig. 3b), one can begin to see PL peaks from uncoupled QDs; we note that they all move together in the same way with temperature as does the empty cavity mode, but at a rate much faster than that mode. Therefore, a QD transition can be temperature-scanned through the cavity resonance[27]. Figure 3b shows an anti-crossing of one QD transition with the cavity mode at 1,182.6 nm. The two normal modes repel each other in the vicinity of the crossing of the red and blue lines, showing the temperature dependence of the uncoupled QD and cavity mode resonances, respectively.

In Fig. 3c, the two coupled-system peaks are plotted as a function of temperature on an expanded wavelength scale; for zero detuning where the uncoupled dot and nanocavity resonances are degenerate, the coupled system emission is clearly double-peaked. This anti-crossing behaviour is characteristic of true strong coupling, the regime of reversible exchange of energy back and forth between the SQD and the nanocavity—that is, vacuum Rabi oscillations.

Figure 4a shows an independent scan over a narrower temperature range close to zero detuning. The measured zero detuning vacuum Rabi splitting is $2g = 41$ GHz $= 170$ μeV $= 0.192$ nm. Figure 4b displays the zero-detuning emission predicted by an analytic expression[28]. There is some uncertainty in the values of κ and γ, and even more in the location of the QD relative to the field maximum. For the plot, $g = 20.6$ GHz; assuming that the dot is in the field maximum, this corresponds to $\mu = 29$ D and a radiative lifetime of 1.82 ns (ensemble measurements gave 1–2 ns).

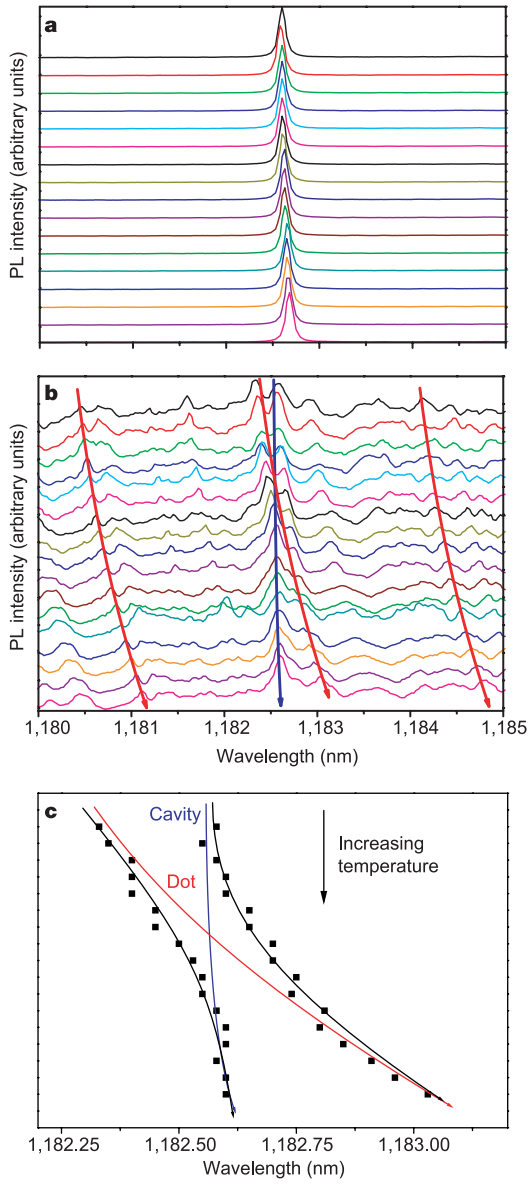

Figure 3 Dot–nanocavity anti-crossing. Temperature is scanned from 13 K at the top to 29 K at the bottom, in 1 K steps. **a**, PL for high excitation power (690 μW) and 0.2 s averaging time; $Q \approx 13{,}300$. The background QD ensemble emission is ~8% of the peak cavity emission here, and ~50% in **b**. **b**, PL at low power (0.78 μW) and 60 s. **c**, The two coupled-system peaks (black lines are guides for the eye) are plotted as a function of temperature, and compared with the scan rates of an uncoupled QD (red curve) and an empty cavity (blue curve).

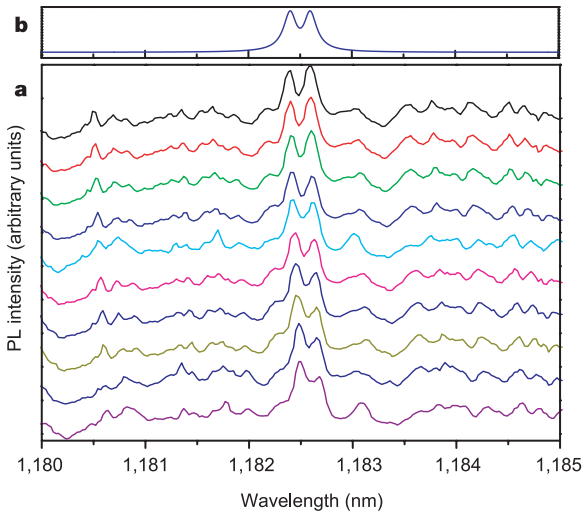

Figure 4 Dot–nanocavity vacuum Rabi splitting. **a**, Near-zero-detuning PL spectra (different run from Fig. 3b), showing double-peaked emission. Temperature is scanned in 0.5 K steps, from 15 K at the top to 19.5 K at the bottom; 0.78 μW and 60 s average. **b**, Plot of analytic expression for zero-detuning emission using $g = 20.6$ GHz $= 0.096$ nm, $\kappa = 42.3$ GHz $= 0.197$ nm, $\gamma = 21.5$ GHz $= 0.1$ nm.

Even though $\sim 10^7$ photons per second are emitted by the coupled system at low power, the signal is weak because most of them stay in the slab; detection through a waveguide coupled to the nanocavity would be far better. If we indeed had only one SQD, there would be little emission from the cavity peak for dot–cavity detunings larger than g; it occurs because of the high density of weakly coupled QDs. Note that the emission spectrum of a strongly coupled system is double-peaked in all directions, unlike that of a quantum-well planar microcavity, which is double-peaked in the nonperturbative-regime, perpendicular direction while single-peaked in the weak-coupling-regime, in-plane direction[29]. This means that the energetic position of the emission peaks should be independent of detection direction.

The anti-crossing of Fig. 3b was observed many times by cycling the temperature. In a new sample, we have seen another clear anti-crossing at 1,214.3 nm with vacuum Rabi splitting $2g = 22$ GHz. We have also seen the weak coupling regime of Purcell enhancement of spontaneous emission: temperature scanning causes the QD resonance to cross straight through the cavity resonance, but coupling increases the radiative linewidth.

We expect that our dot/nanocavity system will exhibit truly quantum effects, although the linear spectroscopy that we report here has not proved this. In contrast, even though the normal-mode coupling seen between a single quantum well and a microcavity also results in a two-peaked anti-crossing and is often called strong coupling by the semiconductor community, it is actually semi-classical—much like many-atom vacuum Rabi splitting[10]. Even a quantum-well three-dimensional microcavity with a mode diameter of only $\sim 2\,\mu$m still requires $\sim$300 photons to saturate its vacuum Rabi splitting; thus it is still semi-classical, and far from the quantum regime[30].

There are at least two advantages of semiconductor QD cavity QED over atomic cavity QED. First, the dot position is fixed; the ability to do experiments with one and the same quantum emitter is essential for both interesting physics and applications in quantum information science. Second, the ultra-small size of the strongly coupled dot/cavity device, with $>10{,}000$ cavities mm^{-2}, allows us to speculate about a quantum network that would be able to store, process and distribute quantum information. The interconnections would be made by photonic crystal waveguides (missing lines of holes). The essential element of a quantum network is a deterministic strong coupling of a single dot to a high-finesse optical photonic crystal cavity—as demonstrated here. □

Received 7 August; accepted 19 October 2004; doi:10.1038/nature03119.

1. Berman, P. (ed.) *Cavity Quantum Electrodynamics* (Academic, San Diego, 1994).
2. Brune, M. *et al.* Quantum Rabi oscillations: A direct test of field quantization in a cavity. *Phys. Rev. Lett.* **76,** 1800–1803 (1996).
3. Haroche, S. Entanglement, decoherence, and the quantum/classical boundary. *Phys. Today* 36–42 (July 1998).
4. Raimond, J. M., Brune, M. & Haroche, S. *Colloquium*: Manipulating quantum entanglement with atoms and photons in a cavity. *Rev. Mod. Phys.* **73,** 565–582 (2001).
5. Mabuchi, H. & Doherty, A. C. Cavity quantum electrodynamics: Coherence in context. *Science* **298,** 1372–1377 (2002).
6. McKeever, J., Boca, A., Boozer, A. D., Buck, J. R. & Kimble, H. J. Experimental realization of a one-atom laser in the regime of strong coupling. *Nature* **425,** 268–271 (2003).
7. Keller, M., Lange, B., Hayasaka, K., Lange, W. & Walther, H. Deterministic coupling of single ions to an optical cavity. *Appl. Phys. B* **76,** 125–128 (2003).
8. Kreuter, A. *et al.* Spontaneous emission lifetime of a single trapped Ca^+ ion in a high finesse cavity. *Phys. Rev. Lett.* **92,** 203002 (2004).
9. Wallraff, A. *et al.* Strong coupling of a single photon to a superconducting qubit using circuit quantum electrodynamics. *Nature* **431,** 162–167 (2004).
10. Khitrova, G., Gibbs, H. M., Jahnke, F., Kira, M. & Koch, S. W. Nonlinear optics of normal-mode-coupling semiconductor microcavities. *Rev. Mod. Phys.* **71,** 1591–1639 (1999).
11. Yablonovitch, E. Inhibited spontaneous emission in solid-state physics and electronics. *Phys. Rev. Lett.* **58,** 2059–2062 (1987).
12. Painter, O. *et al.* Two-dimensional photonic band-gap defect mode laser. *Science* **284,** 1819–1821 (1999).
13. Akahane, Y., Asano, T., Song, B.-S. & Noda, S. High-Q photonic nanocavity in a two-dimensional photonic crystal. *Nature* **425,** 944–947 (2003).
14. Marzin, J.-Y., Gérard, J.-M., Izraël, A., Barrier, D. & Bastard, G. Photoluminescence of single InAs quantum dots obtained by self-organized growth on GaAs. *Phys. Rev. Lett.* **73,** 716–719 (1994).
15. Brunner, K., Abstreiter, G., Böhm, G., Tränkle, G. & Weimann, G. Sharp-line photoluminescence and two-photon absorption of zero-dimensional biexcitons in a GaAs/AlGaAs structure. *Phys. Rev. Lett.* **73,** 1138–1141 (1994).
16. Gammon, D. & Steel, D. G. Optical studies of single quantum dots. *Phys. Today* 36–41 (October 2002).
17. Weisbuch, C., Nishioka, M., Ishikawa, A. & Arakawa, Y. Observation of the coupled exciton-photon mode splitting in a semiconductor quantum microcavity. *Phys. Rev. Lett.* **69,** 3314–3317 (1992).
18. Gammon, D., Snow, E. S., Shanabrook, B. V., Katzer, D. S. & Park, D. Fine structure in the optical spectra of single GaAs quantum dots. *Phys. Rev. Lett.* **76,** 3005–3008 (1996).
19. Petroff, P. M., Lorke, A. & Imamoglu, A. Epitaxially self-assembled quantum dots. *Phys. Today* 46–52 (May 2001).
20. Zrenner, A. *et al.* Coherent properties of a two-level system based on a quantum-dot photodiode. *Nature* **418,** 612–614 (2002).
21. Moreau, E. *et al.* Single-mode solid-state single photon source based on isolated quantum dots in pillar microcavities. *Appl. Phys. Lett.* **79,** 2865–2867 (2001).
22. Bayer, M. *et al.* Inhibition and enhancement of the spontaneous emission of quantum dots in structured microcavities. *Phys. Rev. Lett.* **86,** 3168–3171 (2001).
23. Happ, T. D. *et al.* Enhanced light emission of $In_xGa_{1-x}As$ quantum dots in a two-dimensional photonic-crystal defect microcavity. *Phys. Rev. B* **66,** 041303(R) (2002).
24. Vahala, K. J. Optical microcavities. *Nature* **424,** 839–846 (2003).
25. Santori, C., Fattal, D., Vučković, J., Solomon, G. S. & Yamamoto, Y. Indistinguishable photons from a single-photon device. *Nature* **419,** 594–597 (2002).
26. Yoshie, T., Shchekin, O. B., Chen, H., Deppe, D. G. & Scherer, A. Planar photonic crystal nanolasers (II): Low-threshold quantum dot lasers. *IEICE Trans. Electron.* **E87-C,** 300–307 (2004).
27. Kiraz, A. *et al.* Cavity-quantum electrodynamics using a single InAs quantum dot in a microdisk structure. *Appl. Phys. Lett.* **78,** 2932–2934 (2001).
28. Carmichael, H. J., Brecha, R. J., Raizen, M. G., Kimble, H. J. & Rice, P. R. Subnatural linewidth averaging for coupled atomic and cavity-mode oscillators. *Phys. Rev. A* **40,** 5516–5519 (1989).
29. Stanley, R. P., Houdré, R., Weisbuch, C., Oesterle, U. & Ilegems, M. Cavity-polariton photoluminescence in semiconductor microcavities: Experimental evidence. *Phys. Rev. B* **53,** 10995–11007 (1996).
30. Lee, E. S. *et al.* Saturation of normal-mode coupling in aluminium-oxide-aperture semiconductor nanocavities. *J. Appl. Phys.* **89,** 807–809 (2001).

Acknowledgements The Caltech group thanks S. Noda and Y. Akahane for discussions on the cavity designs, and the MURI Center for Photonic Quantum Information Systems (ARO/ARDA), NSF-ECS-NIRT and AFOSR for financial support. The Tucson group thanks E. Yablonovich for suggestions, and AFOSR, DURINT, NSF-AMOP and NSF-ECS-EPDT for support. The Texas group acknowledges support from NSF-ECS-NIRT.

Competing interests statement The authors declare that they have no competing financial interests.

Correspondence and requests for materials should be addressed to G. K. (galina@optics.arizona.edu).

Current-induced resonance and mass determination of a single magnetic domain wall

Eiji Saitoh[1], Hideki Miyajima[1], Takehiro Yamaoka[2] & Gen Tatara[3]

[1]*Department of Physics, Keio University, Yokohama, 223-8522, Japan*
[2]*SII NanoTechnology Inc., Matsudo, 270-2222, Japan*
[3]*Department of Earth and Space Science, Osaka University, Osaka, 560-0043, Japan*

A magnetic domain wall (DW) is a spatially localized change of magnetization configuration in a magnet. This topological object has been predicted to behave at low energy as a composite particle with finite mass[1]. This particle will couple directly with electric currents as well as magnetic fields, and its manipulation using electric currents[2–8] is of particular interest with regard to the development of high-density magnetic memories[9]. The DW mass sets the ultimate operation speed of these devices, but has yet to be determined experimentally. Here we report the direct observation of the dynamics of a single DW in a ferromagnetic nanowire, which demonstrates that such a topological particle has a very small but finite mass of 6.6×10^{-23} kg. This measurement was realized by preparing a tunable DW potential in the